Precision Passive Mechanical Alignment of Wafers

Alexander H. Slocum, Alexis C. Weber

Precision Engineering Research Group, Massachusetts Institute of Technology,
77 Massachusetts Ave, Room 3-445, Cambridge, MA 02139, slocum@mit.edu

Abstract **- A passive mechanical wafer alignment technique, capable of micron and better alignment accuracy, was developed, fabricated and tested. This technique is based on the principle of elastic averaging: It uses mating pyramids (convex) and grooves (concave) elements, which have been previously patterned on the wafers, to passively align wafers to each other as they are stacked. The concave and convex elements were micromachined on 4 inch (100) silicon wafers using wet anisotropic (KOH) etching and deep reactive ion etching. Repeatability and accuracy 1 μm and better was shown through testing. Repeatability and accuracy were also measured as a function of the number of engaged features. Sub-micrometer repeatability was achieved with as little as 8 mating features. Potential applications of this technique are precision alignment for bonding of multi-wafer MEMS devices and 3-D interconnect IC's, as well as one-step alignment for simultaneous bonding of multiple wafer stacks. Future work will focus on minimizing the size of the features.**

Index Terms **– wafer alignment, kinematic coupling, elastic averaging**

I. INTRODUCTION

Sub-micron alignment for wafer bonding applications has become a major limitation in the development of multi-wafer MEMS devices and 3D interconnects [1,2]. Most wafer alignment is done by mechanically positioning one wafer with respect to another using optical measurement techniques, but the large structural loop[1] makes alignment better than 1 micron difficult, and multi wafer stacks must be assembled one at a time. Passive alignment is used extensively for alignment of optical fibers in MOEMS [3,4,5], and has been used in setups for "rough" wafer-to-wafer alignment [6], and in MEMS packaging applications [7].

Capillary forces at the wafer-air interface between hydrophobic features patterned on wafers can align two wafers to each other to the micron level [8], but would be impractical for a stack of wafers. This paper describes a methodology used to passively align wafers using the principle of elastic averaging.

II. PRECISION ALIGNMENT PRINCIPALS

The design and manufacture of precision instruments and machines has a rich history that emphasized the use of fundamental principles of alignment in order to continually create machines more accurate than those available [9]. Two primary alignment techniques come to mind, kinematic and elastic averaging [10]. The former requires a system to be statically determinant (number of contact points equal number of degrees of freedom restrained). The latter assumes the system is grossly over constrained, but each contact element is relatively flexible, and when forces are applied to clamp the system, the elements deform elastically and errors average.

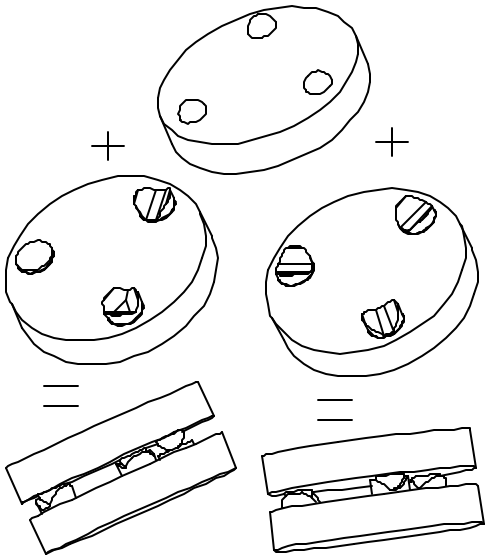

Figure 1: *An object with three hemispheres (top-center) can be deterministically and repeatably coupled to another object with either three v-grooves (middle-right) or with a flat, a v-groove and a trihedral feature (middle left) to create a deterministic kinematic coupling (bottom left and bottom right)*

There are many references to instruments designed as kinematic, or "exact constraint" systems [11,12,13]. These often use a kinematic coupling between the elements. Figure 1 shows two such variants: a three-groove kinematic coupling, which was used by Maxwell to align components in his experiments with light, and three hemispheres mated against a flat plat, a trihedral socket, and a v-groove that pointed towards the socket which was used by Lord Kelvin. The detailed analysis methods for creating kinematic couplings between components are now well known [14,15] where even factors such as friction between surfaces can be overcome with the use of flexural elements to provide compliance in the direction of friction forces, while maintaining high normal stiffness [16].

The principle of *elastic averaging* states that to accurately locate two surfaces and support a large load,

[1] The structural loop is the complete load path through the system, and hence when optically aligning wafers, the structural loop includes the path from one wafer, through the chuck and the machine to the other wafer.

there should be a very large number of contact points spread out over a broad region. Examples include curvic or Hirth couplings, which use meshed gear teeth (of different forms respectively) to form a coupling. The teeth are clamped together with a very large preload. This mechanism is commonly used for indexing tables and indexing tool turrets. A more common example is that of a *wiffle tree* which is the structure that provides support to a windshield wiper. Figure 2 shows the principle as it would be used to allow a single point of loading to apply an even force to 32 devices (e.g., for testing packaged semiconductor devices). An example of the principle of elastic averaging taken to its extreme limit is the structure of the gecko's feet. These animals' feet are covered with hairs, which continue to subdivide at their ends to the microscopic level where they each then can make intimate contact with a surface so Van der Waals forces enable the gecko to stick to smooth surfaces [17].

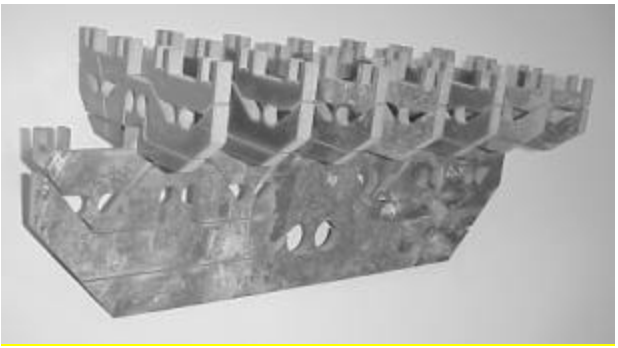

Figure 2*: A 3-D Wiffle tree structure*

There are few references to instruments where precision alignment is attained by elastic averaging, perhaps because the analysis is often intractable, or perhaps because using this method implies a higher risk; however, recently the principle was applied to a new type of shaft coupling [18]. In addition, an interesting elastic averaging effect in silicon was obtained by Han who created "silicon Velcro" that can act as a surface adhesive using thousands of interlocking features [19].

Thus we approached the problem of aligning wafers from the perspective of investigating the possibility of using kinematic or elastic averaging principles, or perhaps even a hybrid system. The first step being a series of experiments to investigate what sort of features might be formed on a wafer to enable an elastic averaging approach. Accordingly, we turned to a very common product used to stack objects together: Lego™ blocks.

III. ELASTIC AVERAGING BENCH LEVEL EXPERIMENT

A series of experiments were performed on Lego™ Duplo™ blocks to quantitatively evaluate the repeatability that can be obtained through the principle of elastic averaging. Lego™ toy building blocks have a set of convex features, or primary projections (PP) and concave features, or secondary projections (SP), which are designed to engage with each other. When two blocks are stacked on top of each other and are preloaded, a small interference fit between the relatively high compliant mating features creates the necessary frictional force to keep the blocks fixed to each other [20].

Lego™ blocks of 8 and 6 PP were repeatedly assembled to each other. The absolute position of the top and the bottom block was recorded at every assembly cycle. The assembly's repeatability was calculated as the total range of the block's position[2]. This experiment was run on three different set-ups. First, the position of the blocks was taken with a Coordinate Measurement Machine (CMM). Capacitive probes were used in the second and third set-ups because of their higher resolution over the CMM[3]. In the second set-up a thin aluminum sheet glued to the blocks was used as a target for the capacitive probes. These blocks were replaced by chrome plated blocks in the third set-up, as shown in Figure 3. Using the chrome-plated blocks reduced Abbe errors, as well as errors caused by relative motion of the aluminum sheets to the blocks.

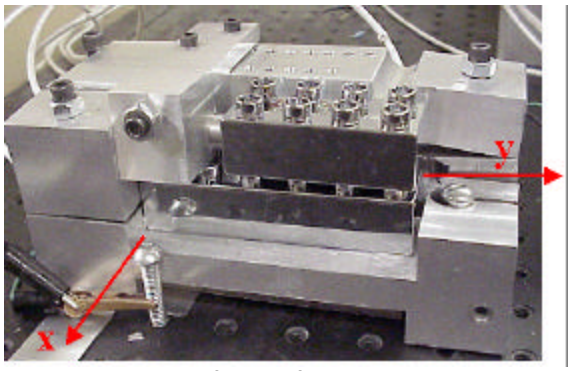

Figure 3*: Set-up used for the first bench level experiment*

Table 1 shows the results of these experiments, as defined in Figure 4, for a 30 cycle long assembly-disassembly run. The repeatability of the measurement system using the third set-up was determined to be of the order of 0.1 μm. The non-zero repeatability of the bottom block is attributed to creep and thermal induced stress. It was expected that **Ty** (repeatability of top block in the y direction) be better than **Tx**, (repeatability of top block in the x direction), since repeatability is typically thought to be inversely proportional to the square root of the number of contact points, and more contact points lie along the y direction then along the x direction of the blocks. However, this was not the case; it is believed that the Abbe error caused by the blocks' aspect ratio, dominates the total error. Thus the relationship between the number of contact points and the magnitude of the error was indistinguishable.

[2] The data taken with the capacitive probes was normalized to the average position for each probed face.

[3] Resolution of capacitive probes ~ 0.05μm vs. ~ 5μm for the CMM.

Nevertheless, the repeatability values obtained are quite impressive and the overall system provided good insight into how a wafer coupling system should be designed.

Set-up	Bx	Tx	By	Ty	Bz	Tz
CMM	5	19	5	20	5.3	20.3
Capacitive, using bonded sheet target	4.7	14.5	4.5	27.4	N/A	N/A
Capacitive, using chrome-plated blocks	1.8	3.4	1.2	4.5	N/A	N/A

Table 1: *Repeatability of 2 by 4 PP Lego™ block, in [mm]*

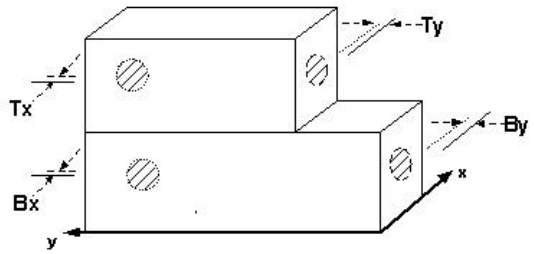

Figure 4*: Probe position and target nomenclature used in bench level experiment*

A second bench level experiment was developed to evaluate the relationship between the number of contact points and the repeatability of an elastically averaged coupling. The set-up used, shown in Figure 5, allows the number of engaged primary and secondary projections between two monolithic target blocks to be varied. The relatively stiff monolithic blocks, comprised of individual, Lego™ blocks[4] that were expoxied together, were assembled repeatedly while recording the top and the bottom blocks' absolute position. Two to five Lego™ blocks, each with 2 by 6 PP were placed between the monolithic blocks to vary the number of contact points by which the monolithic blocks are engaged. Figure 6 shows the set-up with 72 (2 Lego™ blocks) and 180 contact points (5 Lego™ blocks) respectively.

The fixture used in this experiment, shown in Figure 5, consists of a base to which the capacitive probes are fixed to by means of flexural clamps, and a detachable plate, to which one of the monolithic block has been epoxied.

Both parts of the fixture are coupled to each other by a canoe-ball type[5] three groove kinematic coupling. A two-piece set-up is used to allow remote assembly and disassembly of the monolithic blocks[6].

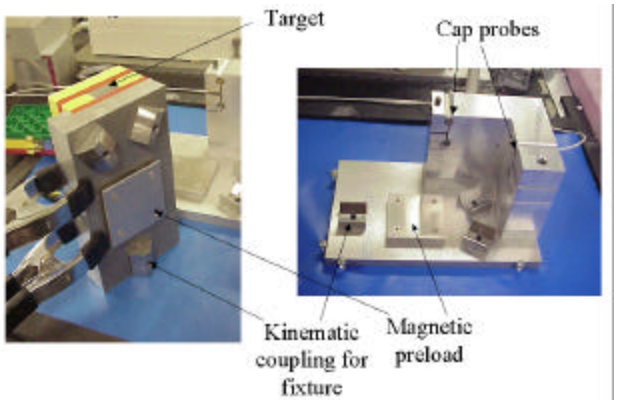

Figure 5*: Second bench level experiment set-up*

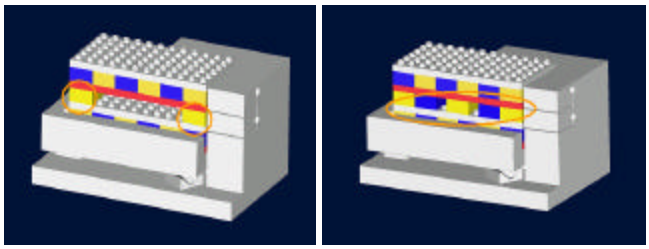

Figure 6*: Second bench level experiment set-up, 72 contact points (left figure) and 180 contact points (right figure)*

The detachable plate can be tilted away from the base, which contains the capacitive probes, to a safe distance for block assembly and disassembly. The kinematic coupling allows the detachable plate to return to the original position relative to the base with very high repeatability. "Canoe ball" kinematic couplings have shown to provide sub micron repeatability when subject to heavy preloads. The preload for the kinematic coupling in this experiment is provided by the mass of the top fixture and by two permanent magnets fixed to the top and the bottom parts of the fixture. Sub-micron repeatability of the measurement system, as shown in Table 2, was determined with this set-up. The set-up was placed in an insulating chamber to reduce errors due to thermal expansion. Table 3 shows the results of a 25 cycle assembly-disassembly run varying the number of contact points.

As expected, both repeatability and standard deviation improve as the number of contact points increases. The theory of random errors would indicate that the repeatability of an elastically averaged coupling is inversely proportional to the number of contact points. Although this is not reflected quantitatively, the experimental results clearly show this trend qualitatively.

[4] Chrome plated blocks were epoxied in the monolithic blocks and used as targets for the capacitive probes.

[5] Instead of using three balls, three surfaces with local radii of contact of 0.25 m, which were ground on a CNC grinding machine, were used so the stiffness and load capacity (preloadability) of the interface are two orders of magnitude greater than for balls. We use these modular canoe-ball coupling elements in our lab because they are far less likely to be damaged by professors in the lab.

[6] The capacitive probes are spaced less than 1mm away from the monolithic blocks; the two-piece set-up prevents physical contact with the probes which causes unwanted drift in the measurements.

	Bx	By	Tx	Ty
Repeatability [μm]	0.56	0.52	0.23	0.85

Table 2: *Repeatability of measurement system (2nd bench level experiment)*

Experiment	X	Y	X st. dev.	Y st. dev.
2 blocks (72 ctct. pts.)	8.15	10.95	2.484	2.759
4 blocks (144 ctct. pts.)	5.47	6.23	1.271	1.737
5 blocks (180 ctct. pts.)	2.80	3.59	0.768	1.021

Table 3: *Repeatability (mm) of 2nd bench level experiment*

IV. PASSIVE WAFER ALIGNMENT STRATEGY

Kinematic couplings and elastically averaged systems are well known to the precision macro world, and hence these principles were applied to create a passive mechanical alignment technique that makes use of matching convex and concave wafer integral features [21]. Given that a kinematic coupling ideally requires high precision compound angled surfaces, which are extremely difficult, if not impossible, to create in silicon wafers, and given the design development in [22], as well as the observations that Lego™ construction bricks seem to fit together well, it was hypothesized that the wafer-to-wafer alignment system could be created based on the concept of elastic averaging using a multitude of structures that might otherwise be used in a kinematic coupling.

The concave alignment structures, shown in Figure 7, consist of eight arrays (two per wafer edge) of 22 KOH etched pyramid-structures mounted on the tip of cantilever flexures [21].

Figure 7*: Solid model of the of convex structures (left); Detail of convex structure (right)*

The convex structures consist of matching arrays of v-grooves patterned on a boss, shown in Figure 8. When the two wafers are stacked upon each other, vibrated lightly and preloaded, the interface between the v-groove and the pyramid causes the flexures to bend. The mating structures self-align the wafers achieving an elastic averaging effect as also shown in the assembled state in Figure 8.

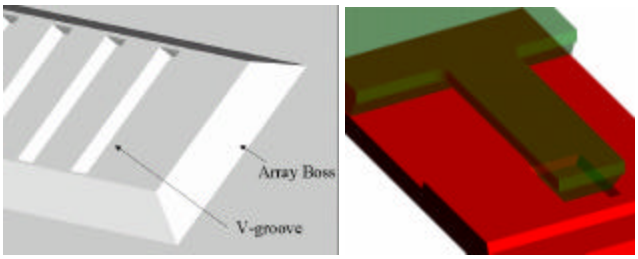

Figure 8*: The boss and v-groove arrays of the concave structures (left) and of the assembled structures (right)*

V. DESIGN OF ALIGNMENT FEATURES

Table 4 presents the dimensions of both concave and convex features. Both features are sized to minimize wafer intrusion while keeping the cantilever strain below 0.2% for a 150μm cantilever tip deflection. The pyramids are sized such that a compact convex corner compensating structure (CCCS), shown in Figure 9 and designed after [23], can be fitted between the pyramids. The CCCS is needed to prevent beveling of the pyramid's convex corners.

Feature	Mask	Size
Pit length	M-1	7 000
Pit width	M1	26 000
Pit distance from wafer center line (inner edge)	M-1	7 500
Cantilever length	M-1 M-2	5 260
Cantilever width	M-2	1 400
Cantilever thickness	M-2	200-250
Pyramid size, at the pyramids top	M-1	1 072
Pyramid size, at the pyramids base	M-1	1 450
CCCS outer rectangle	M-1	2 000
V-groove width	F-1	1 142
V-groove length	F-1	1 900

Table 4: *Concave and convex element feature sizes (mm)*

Generous radii were patterned on the cantilevers' bases during the DRIE step to prevent stress concentration. A halo-mask was used during the DRIE step to shorten the process time and to maintain a constant etch rate throughout the whole wafer.

VI. MICROFABRICATION

3-μm feature size alignment marks are patterned on the wafer front side (for convex feature wafers) and the wafer back side (for concave feature wafers) of 4-inch double-sided polished (100) silicon wafers. The convex features were fabricated with a backside KOH timed etch, which created a 300μm deep pit that defined the cantilever thickness and the pyramid structures. A front-side DRIE released the cantilevers. The concave features were bulk

micro-machined through a single timed KOH etch, which thinned out most of the wafer, leaving eight bosses with an equal number of v-groove arrays.

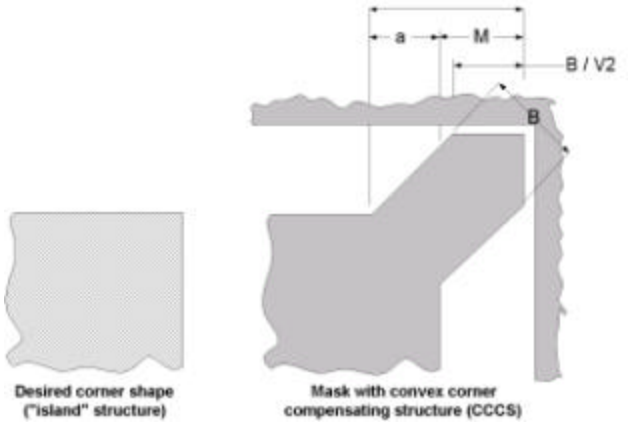

Figure 9*:Convex Corner Compensating Structure (CCCS)*

Figures 10 and 11 show SEM pictures of the convex coupling features and array, as seen from the bottom of the wafer. Note in Figures 10 and 11, that although CCCS were used to mask this wafer, the convex pyramid corners are beveled. This wafer was purposely over-etched during the timed KOH etch to ensure no traces of the CCCS would be present, which could interfere between the convex and the concave features during wafer assembly.

Figure 10: *Convex feature: Pyramid on cantilever's tip*

Figure 12 shows a close up view of the boss and v-grooves or concave structures.
The alignment marks were patterned with a standard e-beam written mask. The KOH etches of both concave and convex structures, as well as the DRIE steps were patterned using masks made from emulsion transparencies

Figure 11: *Array of convex structures, side view*

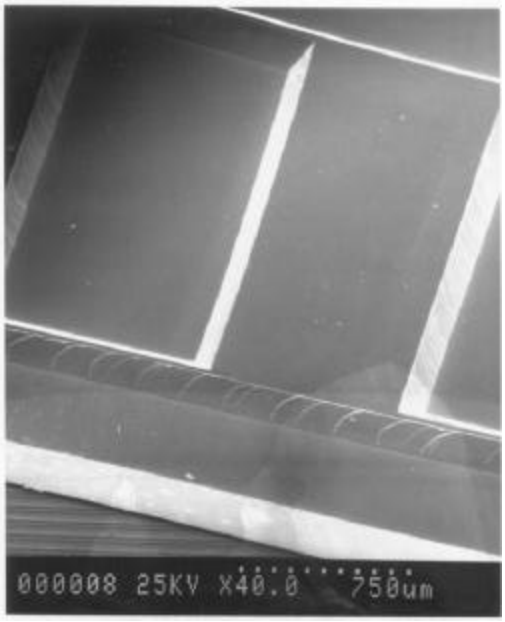

Figure 12: *Array of concave structures, notice boss and v-trenches*

VII. TESTING PASSIVE ALIGNMENT FEATURES

Testing of the passive wafer alignment features was done on an Electronics Vision Group™ TBM8™ wafer alignment inspection system, as shown in Figure 13. Two stacked wafers were mounted on the TBM8™, aligned roughly and tapped lightly to help the wafer alignment features engage and self-align the wafers. After the top wafer had reached a stable position (i.e. would not move when lightly tapped),

the front-to-back side alignment accuracy was measured. The wafer was then removed and put back on many times so repeatability could be determined. Sub micron repeatability and accuracy in the order of 1 μm were shown through testing. Table 5 shows the performance of the measurement system as determined through a "cap test", whereby a wafer was coupled and not removed, while its position was measured many times. Figure 14 shows the nomenclature used for the wafer level experiment results.

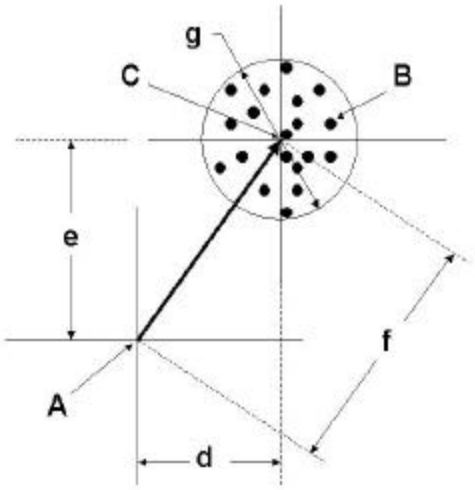

Figure 14: Nomenclature used for wafer level experiments; **A**: bottom wafer alignment mark position (BWAM) used as reference; **B**: top wafer alignment mark position (TWAM) at a particular assembly cycle; **C**: average position of all TWAM (accuracy); **d**, **e** accuracy in X and Y direction; **f**: error vector magnitude; **g**: repeatability. The repeatability in X and Y is taken as the range of TWAM data in each direction respectively. The error vector repeatability is calculated as the range of the magnitude of the error vectors

Table 6 shows the results of a 20-cycle assembly and disassembly sequence, where all 96 cantilever/pyramid elements are used. The grooves showed signs of wear after many dozens of couplings, so a second set of wafers was used for experiments where the cantilevers were to be successively broken off. During this experiment repeatability and accuracy were measured as a function of the number of engaged features. Sub-micrometer repeatability was achieved with as little as 8 mating features. Table 7 shows repeatability and accuracy as a function of the number of engaged features. The offset between repeatability and accuracy is assumed to be caused by misalignment of the masks used to pattern the structures. This misalignment is a fraction of the minimum 20 μm feature size of the masks made from emulsion transparencies.

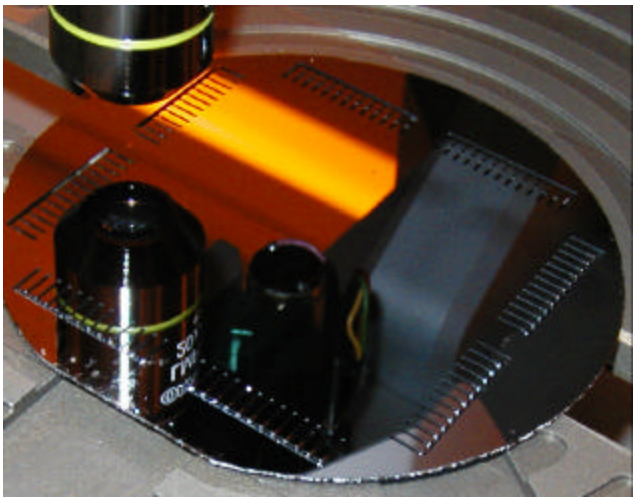

Figure 13: *Testing of the passively mechanically aligned wafers. Notice wafer with convex features lies at the bottom.*

The data shows that the use of many features does not necessarily provide a great increase in accuracy or repeatability as might be expected, but such increases are expected when there are random errors in the elements.

The accuracy error is hypothesized to be systematic in the alignment fiducials, and the repeatability even with only 8 features (two per side) is very good; hence we conclude that wafers can be mechanically aligned to each other using just two of these features per quadrant. This will minimally intrude on the useful wafer surface area.

	X [μm]	Y [μm]	Error [μm]
Accuracy	0.36	-5.31	5.33
Repeatability	0.42	0.42	0.42

Table 5: *Performance of the TBM8™ wafer alignment measurement system, as determined with "cap test".*

	X [μm]	Y [μm]	Error [μm]
Accuracy	0.88	-1.08	1.41
Repeatability	0.63	1.06	1.06

Table 6: *Test results, wafers M-2 and F-1 using, all cantilevers.*

	Total # of cant.	X	Y	Error
Accuracy	96	-6.93	1.35	7.07
Repeatability	96	1.09	0.43	1.12
Accuracy	88	-6.26	0.75	6.3
Repeatability	88	0.84	0.78	0.87
Accuracy	80	-7.29	0.44	7.29
Repeatability	80	0.84	0.84	0.84
Accuracy	72	-1.68	4.52	4.83
Repeatability	72	-1.04	0.85	1.01
Accuracy	64	-4.3	-5.86	7.22
Repeatability	64	0.43	0.42	0.43
Accuracy	56	-5.99	-4.26	7.37
Repeatability	56	0.63	0.21	0.46
Accuracy	48	-6.55	-4.21	7.82
Repeatability	48	0.63	0.42	0.52
Accuracy	40	-6.46	-3.69	7.42
Repeatability	40	0.42	0.63	0.68
Accuracy	32	-4.61	-5.43	7.32
Repeatability	32	0.63	1.05	0.89
Accuracy	24	-7.56	-3.87	8.53
Repeatability	24	0.84	1.05	0.67
Accuracy	16	-7.51	-4.77	8.89
Repeatability	16	0.42	0.64	0.58
Accuracy	8	-7.14	-4.77	8.89
Repeatability	8	0.42	0.89	0.47

Table 7: *Test results (mm) for wafers M-2 and F-2 as a function of reducing the number of cantilevers (contacts) for each test.*

VIII. CONCLUSIONS AND FUTURE WORK

The results of this work validate that it is possible to achieve sub-micron alignment of multi-wafer stacks without the need for optical alignment hardware. Thus this technique can have significant impact in multi-wafer MEMS and stacked 3D IC's. The present implementation does not work for anodic or fusion bonding applications, due to the KOH etch roughness, unless SOI wafers were used. However, we are pursuing design modifications to simplify the design.

Specifically, it is hypothesized that the pyramid structure could also alternatively be formed by an appropriate plated metal structure that would protrude form the surface of a polished wafer and mate with annular structures made by DRIE to form essentially the same type of interface used by Legos™; hence stacks of wafers aligned (coupled) in this manner could then be fusion bonded. In addition, the metal protrusions could be made as surfaces of revolution, which should increase accuracy by reducing edge contacts.

ACKNOWLEDGEMENTS

The microfabrication and testing was carried out at the Microsystems Technology Laboratory at MIT. This research was partially supported by a Grant from the National Science Foundation under Grant # DMI-99002934. The authors wish to thank Delphi Corporation for their generous graduate fellowship support of Alexis Weber.

REFERENCES

1. J. -Q. Lü, et al, "Stacked chip-to-chip interconnections using wafer bonding technology with dielectric bonding glues", Interconnect Technology Conference, 2001. Proc IEEE 2001 Int., 2001, pp. 219-221.

2. A. R. Mirza, "One micron precision, wafer-level aligned bonding for interconnect, MEMS and packaging applications", Electronic Components & Technology Conference, 2000. 2000 Proceedings. 50th, 2000, pp. 676-680.

3. Y. Bäcklund, "Micromechanics in optical microsystems - with focus on telecom systems", *J. Micromech. Microeng*, 7, pp. 93-98, 1997.

4. C. Strandman, et al, "Passive and fixed alignment of devices using flexible silicon elements formed by selective etching", *J. Micromech. Microeng*., 8, pp. 39-44, 1998.

5. R. M. Bostock, et al, "Silicon nitride microclips for the kinematic location of optic fibers in silicon v-shaped grooves*", J. Micromech. Microeng*., 8, pp. 343-360, 1998.

6. R. L. Smith, et al, "A wafer-to-wafer alignment technique", *Sensors and Actuators*, 20, pp. 315-316, 1989.

7. L.-S. Huang, et al, "MEMS packaging for micro mirror switches", *Proc. 48th Electronic Components & Technology Conference*, Seattle, WA. May 1998, pp. 592-597.

8. B. R. Martin, et al, "Self-alignment of patterned wafers using capillary forces at a water-air interface", *J. Adv. Funct. Mater.*, 11, No. 5, pp. 381-386, Oct. 2001.

9. C. Evans, *Precision Engineering: An evolutionary view*, Cranfield, Bedford, MK43 0AL, England: Cranfield Press, 1989, pp. 22-33.

10. A. Slocum, *Precision Machine Design*, Dearborn, MI: SME, 1992, pp. 352-354.

11. R. S. Whipple, "The design and construction of scientific instruments", *Transactions of the Optical Society*, v 22, pp. 3-52, 1920-1921.

12. L. S. Brooks, "Adjustable instrument mount", *J. Opt. Soc. Am.*, v44, p.87, 1954.

13. E. Hog, "A kinematic mounting ", *Astron & Astrophys*, v 41, pp. 107-109, 1975.

14. A. Slocum, "Design of three-groove kinematic couplings", *Precis Eng*., Vol. 14, No. 2, pp. 67-76, April 1992.

15. P. Smeichen, A. Slocum, "Analysis of kinematic systems: a generalized approach", *Precision Eng*., Vol. 19, No. 1, pp.11-18, July 1996.

16. C. H. Schouten, J. N. Rosielle, and P. H. Shellens, "Design of a kinematic coupling for precision applications", *Precision Engineering*, 20(1), pp. 46-52, 1997.

17. K. Autumn, Y. Liang, W.P. Chan, T. Hsieh, R. Fearing, T.W. Kenny, and R. Full, "Dry adhesive force of a single gecko foot-hair", *Nature*, 405, pp. 681-685, 2000.
18. A. Slocum, "Precision machine design: macromachine design philosophy and its applicability to the design of micromachines", IEEE Micro Electro Mechanical Systems '92, Travemunde Germany, Feb. 4-7, 1992, pp. 37-42.
19. H. Han. L. Weiss, M. Reed, "Micromechanical velcro", *Journal of Microelectromechanical Systems*, Vol 1, No.1, pp. 37-43, March 1992.
20. G. K. Christiansen, "Toy Building Brick", US patent 3,005,282, Oct. 1961.
21. A. Slocum, D. Braunstein, L. Muller, "Flexural Kinematic Couplings", US patent 5,678, 944, Oct. 1997.
22. M. Balasubramaniam, H. Dunn, E. Golaski, S. Son, K. Sriram, A. Slocum, "An anti backlash two-part shaft with interlocking elastically averaged teeth", *Precis. Eng.*, Volume 26, No. 3, pp. 314-330, 2002.
23. Q. Zhang, et al, "A new approach to convex corner compensation for anisotropic etching of (100) Si in KOH", *Sensors and Actuators*, A, 56, pp. 251-254, 1996.